Cellulose (2018) 25:5035–5048
https://doi.org/10.1007/s10570-018-1910-4

ORIGINAL PAPER

A novel effective approach of nanocrystalline cellulose production: oxidation–hydrolysis strategy

Oleg V. Surov · Marina I. Voronova · Natalia V. Rubleva · Lyudmila A. Kuzmicheva · Daniil Nikitin · Andrei Choukourov · Valery A. Titov · Anatoly G. Zakharov

Received: 28 February 2018 / Accepted: 14 June 2018 / Published online: 18 June 2018
© Springer Nature B.V. 2018

Abstract In this work, we have applied, for the first time, solution plasma processing of cellulose-containing material to produce cellulose nanocrystals (CNC). The CNC samples produced in three different modes of solution plasma treatment were characterized using methods of dynamic light scattering, infrared spectroscopy, transmission electron microscopy, X-ray diffraction, and X-ray photoelectron spectroscopy. The proposed method of CNC production comprising the oxidation–hydrolysis strategy has proved to be effective and allowed us to reduce significantly the time of acid hydrolysis and to increase considerably the total CNC yield.

Graphical Abstract

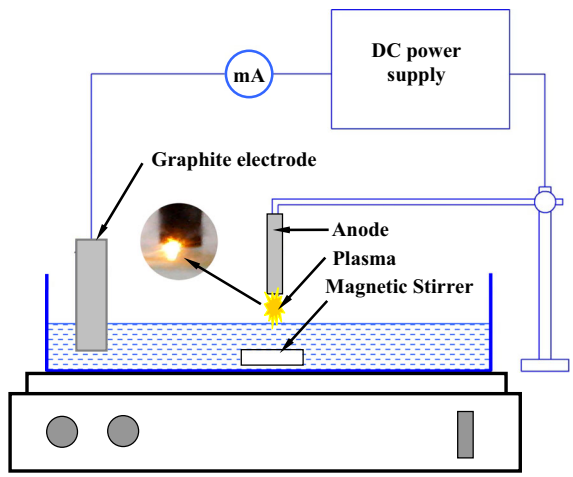

Keywords Cellulose nanocrystals · Oxidation–hydrolysis strategy · Solution plasma processing

Abbreviations

CNC	Cellulose nanocrystals
MCC	Microcrystalline cellulose
FP	Filter paper
DC	Direct current
ζ-potential	Electrokinetical potential
IR-spectroscopy	Fourier transform infrared spectroscopy
DLS	Dynamic light scattering
TEM	Transmission electron microscopy

Electronic supplementary material The online version of this article (https://doi.org/10.1007/s10570-018-1910-4) contains supplementary material, which is available to authorized users.

O. V. Surov (✉) · M. I. Voronova · N. V. Rubleva · L. A. Kuzmicheva · D. Nikitin · V. A. Titov · A. G. Zakharov
G.A Krestov Institute of Solution Chemistry of the Russian Academy of Sciences, 1 Akademicheskaya St., Ivanovo, Russian Federation 153045
e-mail: ovs@isc-ras.ru

D. Nikitin · A. Choukourov
Department of Macromolecular Physics, Faculty of Mathematics and Physics, Charles University, V Holešovičkách 2, 18000 Prague, Czech Republic

XRD	X-ray diffraction
XPS	X-ray photoelectron spectroscopy

Introduction

Cellulose nanocrystals (CNC) generally refer to a type of rod-like cellulose nanomaterial with a typical length of 50–500 nm, a diameter of 3–10 nm, a degree of polymerization between 100 and 300, a moderate density, a high degree of crystallinity and a very high tensile strength and modulus (Zhu et al. 2016; Kargarzadeh et al. 2017; Julkapli and Bagheri 2017). The production of CNC from cellulosic fibers through acid hydrolysis, known for more 6 decades, remains the dominant process nowadays (Mondal 2017). High sulfuric acid concentrations (approximately 62–64 wt%) are commonly used. This is due in part to the formation of sulfate groups that impart electrostatic stability to CNC to facilitate aqueous processing. Typically, higher acid concentrations, longer reaction times, and higher temperatures lead to higher surface charge and narrow particle sizes, but to lower yield and decreased crystallinity and thermal stability of CNC. Different mineral and organic acids can also be used for CNC production, e.g. hydrochloric (Araki et al. 1998; Yu et al. 2013), hydrobromic, phosphoric (Camarero Espinosa et al. 2013; Um et al. 2003), maleic (Filson and Dawson-Andoh 2009), nitric (Liu et al. 2010), formic (Yan et al. 2015), and carboxylic acids (Chen et al. 2016a; Espino-Pérez et al. 2014; Spinella et al. 2016), as well as mixtures of acids (Braun and Dorgan 2008).

Difficulties in economic recovery of acids and low CNC yields (approximately 30 wt%) have been the main drawbacks of using mineral or organic acids for CNC production. Recently, a number of studies have focused on hydrolysis parameter optimization (Bondeson et al. 2006; Hamad and Hu 2010; Wang et al. 2012; Chen et al. 2015; Ioelovich 2012, 2013; Beck-Candanedo et al. 2005; Dong et al. 1998), corrosion prevention, and waste reduction (Mao et al. 2017). Liu et al. (2014) reported preparation of CNC using the hydrolysis of bleached pulp with solid phosphotungstic acid ($H_3PW_{12}O_{40}$). They found that the resultant CNC had a significantly higher thermal stability than the CNC prepared by hydrolysis with sulfuric acid. In addition, the solid acid could be easily recovered and recycled through extraction with diethyl ether. Torlopov et al. (2017a, b) studied the influence of $H_3PW_{12}O_{40}$ concentration, sonication pre-treatment, hydrogen peroxide and octanol-1 addition on the CNC yield, thermal stability, morphology and size of CNC particles.

Kontturi et al. (2016) demonstrated that the use of HCl vapor results in the rapid hydrolysis of cotton-based cellulose fibers under ambient conditions. The authors observed an increase in crystallinity without practically any mass loss in the cellulose substrate during the hydrolysis. They showed how this hydrolysis process can be applied for the facile high-yield production of CNC with minimal water consumption. Generally, various types of gaseous acids can be used in this procedure, such as nitric acid, and trifluoroacetic acid. This technique can allow several environmentally harmful and time-consuming steps that are required for classical acid hydrolysis to be omitted.

Metal inorganic salts have been demonstrated by many researchers for enhancing the hydrolysis efficiency of cellulose (Liu et al. 2009; López-Linares et al. 2013; Zhang et al. 2015) and preparation of micro- or nanocrystalline cellulose (Li et al. 2015; Lu et al. 2014). A transition metal-based catalyst provides a feasible, selective, and controllable hydrolysis process with mild acidity. It was found that the valence state of the metal ion is the key factor to influence the hydrolysis efficiency. A higher valence state generates more H+ ions, which act effectively in the co-catalyzed acid hydrolysis reaction in the presence of metal ions (Yahya et al. 2015; Chen et al. 2016b). The presence of an acidic medium or ultrasonic-assisted treatment can act synergistically to improve the accessibility of metal ions for the hydrolysis process (Karim et al. 2014). Recently, Cheng et al. (2017) used inorganic chlorides, $FeCl_3{\cdot}6H_2O$, $CuCl_2{\cdot}2H_2O$, $AlCl_3$, and $MnCl_2{\cdot}4H_2O$, in hydrochloric acid hydrolysis to extract CNC from microcrystalline cellulose under hydrothermal conditions. They observed the enhanced salt-catalyzed hydrolysis at a relatively low acid concentration through faster degradation of the disordered region of cellulose.

Novo et al. (2015, 2016) showed that subcritical water could promote the hydrolysis of amorphous and semi-crystalline regions of cellulose. It was revealed that the exclusive use of water as a reagent is a

promising process not only for its green characteristics but also for its low corrosion, low and cleaner effluent, and low cost of reagents.

Other CNC preparation techniques include treatment with ionic liquids (Man et al. 2011; Miao et al. 2016; Zhang et al. 2017), enzymatic hydrolysis (Siqueira et al. 2010; Filson et al. 2009), and production by oxidation (Leung et al. 2011; Hirota et al. 2010a, b; Montanari et al. 2005). These techniques are usually applied in combination with other chemical and mechanical or ultrasound treatments. The TEMPO-meditated oxidation method has widely been applied to cellulose fibers to produce CNC. It has been reported that isolated CNC reveal superior dispersity in water after TEMPO oxidation, because of the incorporation of a higher number of carboxylate groups in the cellulose (Hirota et al. 2010a, b; Montanari et al. 2005; Peyre et al. 2015). Recently, solvothermal pretreatment of cellulose with ethanol and peroxide followed by ultrasonic treatment has been used to produce CNC (Li et al. 2016).

On the other hand, in the past decades emerging discharge plasma-based technologies continuously find increasing applications in polymer chemistry, e.g. for a specific surface functionalization of materials without affecting their bulk properties (Khelifa et al. 2016). Moreover, plasma in liquid-phase or solution plasma processing has been recognized as an advanced oxidation process due to its ability to produce highly active species especially hydroxyl radical (Zakharov et al. 2007). Recently, Prasertsunga et al. (2017) studied conversion of microcrystalline cellulose into reducing sugar in diluted sulfuric acid by solution plasma processing.

For the best of our knowledge, in this work for the first time we report the results on plasma-chemical treatment of cellulosic materials (microcrystalline cellulose and filter paper) in solution bulk for CNC production.

Materials and methods

Materials

Commercial microcrystalline cellulose (MCC) (powder, ~20 μm) and Whatman qualitative filter paper (Grade 1) (FP) were purchased from Sigma-Aldrich. Sulfuric acid (chemically pure, GOST 4204-77) was purchased from Chimmed (Russia).

Solution plasma treatment of cellulose

Atmospheric pressure glow discharge with an electrolytic cathode is the simplest type of the plasma-solution system and it was used for the treatment of cellulose suspension in our study. The setup is shown in Fig. 1. Similar setup was used for modification of chitosan in aqueous solution and for the coupling of chitosan onto polypropylene surface (Nikitin et al. 2016).

The occurrence of the glow discharge between the anode in the gas phase and electrolyte solution initiates redox reactions in it. These reactions are mainly triggered by the formation of primary chemically active particles (radicals OH, H, solvated electrons) in the surface layer of the solution under ion bombardment. Despite the small thickness of the surface solution layer (hundredths of a micron), they have enough time to start interacting in this thin layer. In the remaining solution volume, the processes can involve a secondary active product—hydrogen peroxide (Zakharov et al. 2007; Titova et al. 2012; Kuz'micheva et al. 2011, 2012). Here, a direct current (DC) discharge was excited between the graphite anode in the gas phase and the liquid surface being used as a cathode. The discharge gap length was equal to 3 mm, the volume of the solution being treated was 50 mL, and the discharge current (i) was maintained at 40 mA

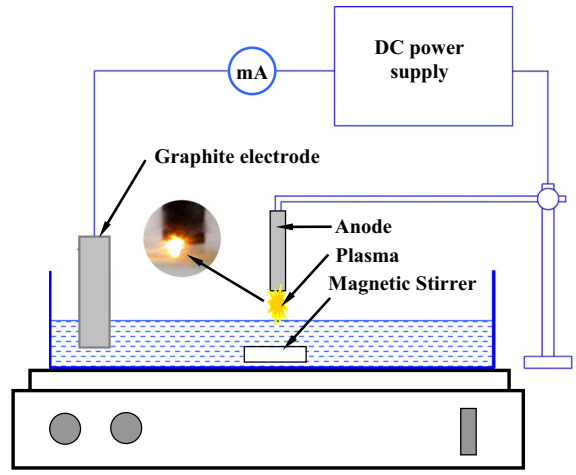

Fig. 1 Schematic diagram of the setup for plasma solution treatment of cellulose

for treatment in distilled water and 20 mA under treatment in sulfuric acid solutions. The processing time was varied in the range of 5–80 min depending on solution composition. The glow discharge voltage was from 305 to 1680 V and the solution temperature was from 22 to 68 °C depending on the processing conditions.

Cellulose treatment was carried out in three different modes: (1) plasma-chemical treatment of MCC and FP of various durations (5–30 min) in sulfuric acid solutions of different concentrations (0.1–64%); (2) preliminary plasma-chemical treatment of MCC and FP of various durations (15 and 30 min) in distilled water followed by sulfuric acid hydrolysis at 50 °C for 2 h (H_2SO_4 concentration of 30–64%); (3) plasma-chemical treatment of CNC aqueous suspension previously produced from MCC by sulfuric acid hydrolysis according to the standard procedure (hydrolysis in 64% H_2SO_4 at 50 ° C for 2 h). We will use the format of (N-XX-YY) to represent experimental conditions of (solution plasma treatment mode, H_2SO_4 concentration in wt%, treatment duration in min) throughout the text.

Characterization of plasma-treated cellulose

The CNC yield in processing modes 1 and 2 was determined gravimetrically. The collected suspension was washed with bidistilled water by repeating centrifugation cycles (10 min, 8000 rpm) until it reached a constant pH value (at least 5–6 washings) and separated on an MN GF-1 filter (Macherey-Nagel, Germany) with particle retention capacity of 0.7 μm. The filtered CNC suspension was collected and its volume was determined. Several parallel samples of accurately measured volume were taken, poured into Petri dishes, which had been weighed in advance, and dried in air till their weight remained constant. Having determined in such a way the suspension concentration and knowing its volume (accounting for the initial cellulose mass), we calculated the CNC yield. The relative error in CNC yield measurement in three parallel experiments did not exceed 2.5%. The part of the suspension that remained in the filter was dried together with the filter. By measuring the weight increase, we determined the mass of the large particles that had not been hydrolyzed. The portion of the soluble hydrolysis products was calculated as the difference between the initial cellulose mass and the total mass of the large particles on the filter and particles in suspension after filtering (CNC).

The films of CNC samples for X-ray diffraction analysis, IR-spectra registration, etc. were obtained by natural evaporation of water at room temperature from aqueous suspensions with the concentration of 10 g/l. Before casting the films, the suspensions were treated with ultrasound (Sonorex DT 100, Bandelin, Germany) for 15 min.

The size of CNC particles was determined using a transmission electron microscope (TEM) "EMV-100L" (Russia) and by the dynamic light scattering method (DLS) using a particle size analyser Zetasizer Nano ZS (Malvern Instruments Ltd, UK) and Analysette 22 (Fritsch GmbH, Germany).

The CNC particle surface charge in aqueous suspension was evaluated by measuring the ζ-potential (Zetasizer Nano ZS).

The CNC polymerization degree was determined based on the viscosity of its solution in cadoxen.

The chemical composition of the films was evaluated by X-ray photoelectron spectroscopy (XPS) (Phoibos 100, Specs, Germany) with an Al Kα X-ray source and a hemispherical energy analyzer. The C_{1s} wide and high-resolution spectra were acquired with a pass energy of 40 and 10 eV to assess the elemental composition and the C_{1s} binding environment, respectively. The spectra were charge referenced for the position of the C−O−C groups at 286.5 eV. The concentration of the surface functional groups was calculated from the deconvolution of the C_{1s} spectra with four components at 285.0 eV (the C−C/C−H groups), 286.5 eV (the C−O−C groups), 287.8 eV (the C=O groups), and 289.0 eV (the O−C=O groups).

The elemental analysis was done on a Flash EA-1112 analyzer (Thermo Quest, Italy) and by using an Oxford Instruments attachment to the scanning electron microscope VEGA3 TESCAN by the method of energy-dispersive X-ray analysis and based on X-ray photoelectron spectroscopy data.

The X-ray diffraction analysis of the films was performed on a Bruker D8 Advance diffractometer (Germany) in the Bragg-Brentano configuration employing Cu-$K\alpha$-radiation ($\lambda = 0.1542$ nm). The scanning angular range was equal to 2°–35° with the scanning step of 0.01°. We used a Vantec-1 high-speed detector. The pulse acquisition time at each scanning point equaled 0.5 s. The crystallinity index was calculated by the Segal method, while the

crystallite sizes were determined by the Scherrer equation (Voronova et al. 2015; Ioelovich 2017).

The IR-spectra were obtained on a VERTEX 80v spectrophotometer (Bruker, Germany) in the wavenumber range of 4000–400 cm^{-1}. The CNC samples compressed into tablets contained 1 mg of the sample to be analyzed and 100 mg of KBr. The measurements were made at room temperature.

UV-Vis spectra of solutions were produced with a SF-100 spectrophotometer (Russia).

NMR experiment was performed on a Bruker Avance III 500 NMR spectrometer equipped with a 5 mm probe using standard Bruker TOPSPIN Software. One-dimensional NMR proton spectra for the water-soluble components with addition of D_2O referenced to TMS were collected at 500 MHz and 25 °C. Water suppression was accomplished using the Watergate pulse sequence (Piotto et al. 1992). Spectra were acquired with a 8 kHz sweep width, 32 K points, and 4096 scans.

Results and discussion

It is known that presence of oxidized (aldehyde or carboxyl) groups in a cellulose macromolecule changes the rate of hydrolysis. Depending on the position of the aldehyde or carboxyl groups in the pyranose heterocycle (at C-2, C-3 or C-6 carbon atom), the rate of hydrolysis can be decreased or increased (Bikales and Segal 1971). We have earlier shown that solution plasma processing at atmospheric pressure employing diaphragm discharge or end discharge increases the total content of aldehyde and carboxyl groups and reduces the degree of cellulose polymerization (Titiova et al. 2008). In this work, we propose a novel approach of producing CNC, namely, oxidation–hydrolysis strategy comprising cellulose oxidation by solution plasma treatment and cellulose hydrolysis by sulfuric acid.

The conditions for plasma-chemical treatment and results of visual inspection are given in Table 1. Table 1 shows values of current intensity, weight ratio of cellulose and solution, acid concentration, the

Table 1 Conditions of solution plasma processing of MCC and FP (0.5 g of cellulose in 50 g of solution): atmospheric pressure DC discharge; T_0 is the initial temperature, T_{pr} is the final processing temperature

Processing format	Processing conditions	Results of visual observation
Mode 1		
1-64-15	64% H_2SO_4, i = 20 mA, T_0 = 22 °C, T_{pr} = 68 °C, t = 15 min	A stable, slightly turbid suspension is formed as a result of MCC treatment. A transparent solution is formed as a result of FP treatment
1-62-15	62% H_2SO_4, i = 20 mA, T_0 = 22 °C, T_{pr} = 68 °C, t = 15 min	Change in color of solution from dark yellow to yellow-brown
1-62-10	62% H_2SO_4, i = 20 mA, T_0 = 22 °C, T_{pr} = 62 °C, t = 10 min	Change in color of solution (yellow)
1-62-5	62% H_2SO_4, i = 20 mA, T_0 = 22 °C, T_{pr} = 46 °C, t = 5 min	Change in color of solution from pale yellow to yellow
1-60-15	60% H_2SO_4, i = 20 mA, T_0 = 22 °C, T_{pr} = 67 °C, t = 15 min	Change in color of solution (pale yellow)
1-55-15	55% H_2SO_4, i = 20 mA, T_0 = 22 °C, T_{pr} = 62 °C, t = 15 min	A slight change in color of solution from pale yellow to yellow
1-30-15	30% H_2SO_4, i = 20 mA, T_0 = 22 °C, T_{pr} = 58 °C, t = 15 min	
1-0.1-15	0.1% H_2SO_4, i = 20 мА, T_0 = 22 °C, T_{pr} = 58 °C, t = 30 min	
Mode 2		
2-0-15	Distilled water, i = 40 mA, T_0 = 22 °C, T_{pr} = 60 °C, t = 15 min	A noticeable swelling of FP
2-0-30	Distilled water, i = 20, T_0 = 22 °C, T_{pr} = 59 °C, t = 30 min	
Mode 3		
3-0-15	Aqueous CNC suspension (3 wt%), 50 g, i = 20 mA, T_0 = 22 °C, T_{pr} = 58 °C, t = 15 min	

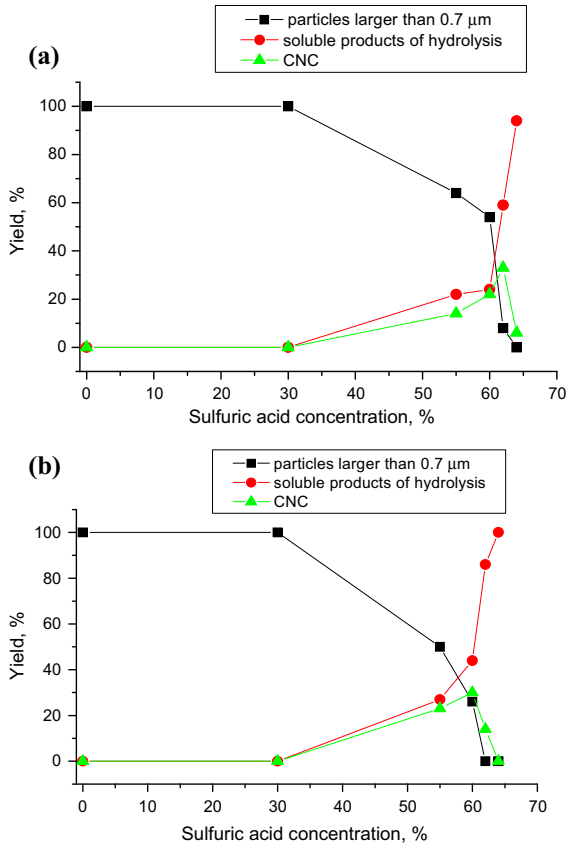

Fig. 2 Results of solution plasma processing of MCC (**a**) and FP (**b**) in sulfuric acid solutions (processing mode 1, the processing duration is 15 min)

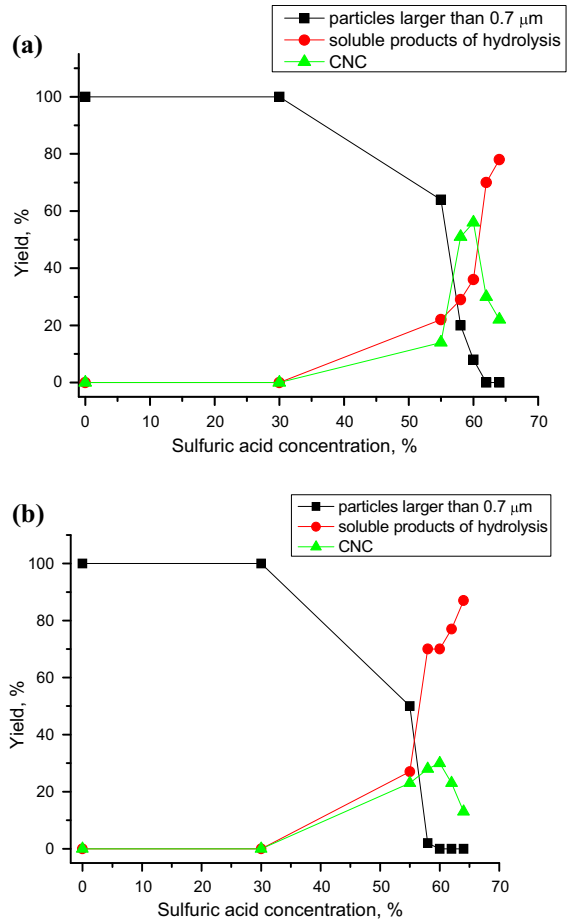

Fig. 3 Results of MCC (**a**) and FP (**b**) processing in mode 2 (the plasma treatment duration is 30 for MCC and 15 min for FP)

processing time, initial and final temperature of the treated cellulose suspension.

Figures 2 and 3 show the results of solution plasma processing of MCC and FP in modes 1 and 2.

Comparison of Figs. 2 and 3 shows that preliminary solution plasma treatment of cellulose followed by sulfuric acid hydrolysis (processing mode 2) almost doubles the yield of CNC (up to 56%) when the starting material is MCC. If the starting material is FP, processing modes 1 and 2 give approximately the same CNC yield ($\sim$30%).

The CNC samples produced in three different modes of solution plasma treatment were characterized by different methods. The obtained characteristics are shown in Tables 2 and 3.

Thus, we have obtained stable CNC suspensions by applying solution plasma processing of MCC and FP. The CNC particles have a typical size of 200–500/30–40 nm (length/width) (Figs. 4, 5) and a sufficiently high charge of the surface (the ζ-potential value is about $-$ 40 mV), which causes the high colloidal stability of these suspensions.

The X-ray diffraction patterns of the CNC films are shown in Fig. 6. The diffraction peak arising at about $2\theta = 22.9$ is attributed to the (200) plane of cellulose I_β whereas the two overlapped weaker diffractions at 2θ close to 14.8° and 16.6° are assigned to the (1–10) and (110) lattice planes of cellulose I_β (French 2014). The CNC films are characterized by a high crystallinity index (81–90) with crystallites of 3.5–5.3 nm in size (Table 2).

The analysis of IR-spectra shows (Fig. 7) that plasma processing of MCC and FP in distilled water leads to cellulose oxidation which becomes apparent in the increasing intensity of the bands around 1730 cm^{-1} and in the region of 1383–1385 cm^{-1}

Table 2 Characteristics of the CNC samples produced in three different modes of MCC and FP processing

Processing format	CNC yield (%)	[a]Degree of polymerization	[b]Hydrodynamic particle size (1st fraction/2nd fraction) (nm)	[c]ζ-potential (mV)	[d]Crystallinity index	[d]Crystallite size (nm)
MCC, mode 1						
1-64-15	6	75	170/25	− 39	86	3.5
1-62-15	33	80	210/30	− 37	89	4.4
1-60-15	22	100	200/30	− 36	88	4.7
1-55-15	14	120	600/95	− 36	88	4.9
FP, mode 1						
1-64-15	0	–	–	–	–	–
1-62-15	14	122	250/30	− 39	83	4.0
1-60-15	30	–	220/40	− 37	87	4.0
1-55-15	23	177	210/40	− 37	87	4.0
MCC, mode 2						
2-64-30	22	80	200/30	− 45	90	4.3
2-62-30	30	85	280/40	− 43	89	4.7
2-60-30	56	92	240/30	− 40	88	4.6
2-55-30	14	130	420/70	− 40	87	5.3
FP, mode 2						
2-64-15	13	79	–	− 40	84	3.8
2-62-15	23	82	–	− 41	85	4.0
2-60-15	30	85	320/70	− 38	86	4.1
2-55-15	23	105	420/95	− 40	85	4.1
MCC, mode 3						
3-0-15	–	80	460/80	− 40	90	5.0
FP, mode 3						
3-0-15	–	86	470/70	− 41	81	4.1

[a]Determined by solution viscosity in cadoxen

[b]Dynamic light scattering method

[c]Determined by Zetasizer Nano ZS

[d]X-ray diffraction analysis

(stretching vibrations of the carboxyl group) (samples 2-0-30 and 2-0-15 for MCC and FP, respectively).

At the same time, the intensity of the 1730 cm^{-1} band in the samples treated in H_2SO_4 is even lower than that in the starting MCC or FP.

Thereupon it is worth noting the following. Cellulose is composed of D-glucose units linked via β-1,4-glycosidic bonds, containing both crystalline and amorphous regions. A great deal of intra- and intermolecular hydrogen bonds enable the molecular structure of cellulose to be fully cross-linked. This kind of special composition and structure causes a challenging problem for cellulose depolymerization as diffusion of proton to β-1,4-glycosidic bonds is one of the essential steps for hydrolysis of cellulose catalyzed by an acid (Rogovin 1972). It has been reported that carboxyl groups on the cellulose chains can serve as catalytically active sites for scission of the neighboring β-1,4-glycosidic bonds in cellulose and the subsequent hydrolysis of cellulose (Zhou et al. 2015; Hirosawa et al. 2001). As a result, the problem of proton diffusion to glycosidic bonds is resolved, and the efficient hydrolysis of cellulose is realized. Most probably, amorphous regions of cellulose are subjected to oxidation in the first place. As a result of subsequent hydrolysis, the oxidized cellulose is

Table 3 Elemental composition and results of analysis of C_{1s} XPS spectra for the CNC samples produced in different plasma-chemical processing modes

Processing format	Elemental composition (%)										[c]Relative content of functional groups (%)			
	[a]H	[a]C	[b]C	[c]C	[a]O	[b]O	[c]O	[a]S	[b]S	[c]S	C–C/C–H	C–O	O–C–O/C=O	O–C=O
MCC, mode 1														
1-55-15	6.66	46.3	40.2	59.5	53.3	33.8	40.1	0.23	0.39	–	25	56	16	3
1-60-15	–	–	55.1	58.3	–	43.2	41.2	–	0.45	–	25	58	15	2
1-62-5	6.35	45.8	41.3	61.6	53.7	35.1	38.4	0.27	0.7	–	30	53	14	3
1-62-10	5.73	45.4	41.6	59.4	53.1	34.3	39.7	0.76	0.93	0.4	24	59	15	2
1-62-15	6.14	45.1	40.3	78.6	53.6	33.7	21.4	1.04	1.26	–	–	–	–	–
FP, mode 1														
1-30-30	6.28	36.6	–	–	42.7	–	–	0.1	–	–	–	–	–	–
1-55-15	–	–	54.5	72.0	35.0	44.9	27.8	–	0.5	–	–	–	–	–
1-62-5	–	–	54.4	57.2	33.6	44.9	42.3	–	0.67	–	21	59	16	4
1-62-15	4.63	40.3	54.1	58.6	–	44.5	40.6	1.03	1.41	0.5	20	64	14	2
MCC, mode 3														
3-0-15	–	–	52.9	57.0	–	44.6	41.6	–	1.37	0.8	23	60	15	2
FP, mode 3														
3-0-15	–	–	53.5	58.9	–	39.6	37.8	–	1.83	1.3	–	–	–	–
Control sample														
H_2SO_4 hydrolysis, standard procedure	–	–	–	58.6	–	–	41.4	–	–	–	17	66	14	3

[a]Determined by a Flash EA-1112 analyser

[b]Determined by the method of energy-dispersive X-ray analysis (VEGA3 TESCAN)

[c]Determined by the X-ray photoelectron spectroscopy (Phoibos 100, Specs)

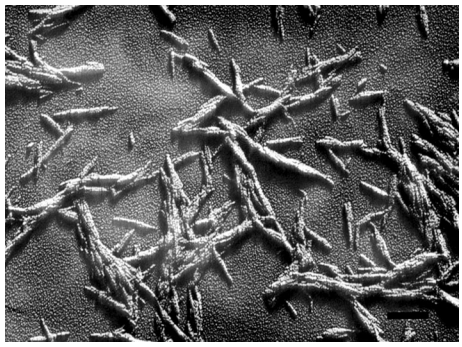

Fig. 4 TEM image of the CNC sample produced from MCC in the 2-60-30 processing format. Scale bar is 100 nm

mainly converted to water-soluble products, promoting the release of CNC particles. Apparently, cellulose surface peeling and partial replacement of the carboxyls by sulfonate groups on the surface of the CNC particles can also occur.

This fact is confirmed by the higher sulfur content under more severe conditions of cellulose treatment (higher acid concentration and longer processing time), while the relative content of oxygen and carbon remains virtually unchanged, as is the relative content of carbonyl and carboxyl groups (Table 3). Unfortunately, the intensity of characteristic bands of the sulfonate groups is very low, and their detection with IR spectroscopy is significantly hampered (Lin and Dufresne 2014; Lu and Hsieh 2010). The relative content of oxygen and carbon varies widely depending on the sample and the method of determination, but on an average their ratio (for the methods analysing the surface) is close to the theoretical value of 0.83 for the surface of pure cellulose (Gaiolas et al. 2009) (Table 3).

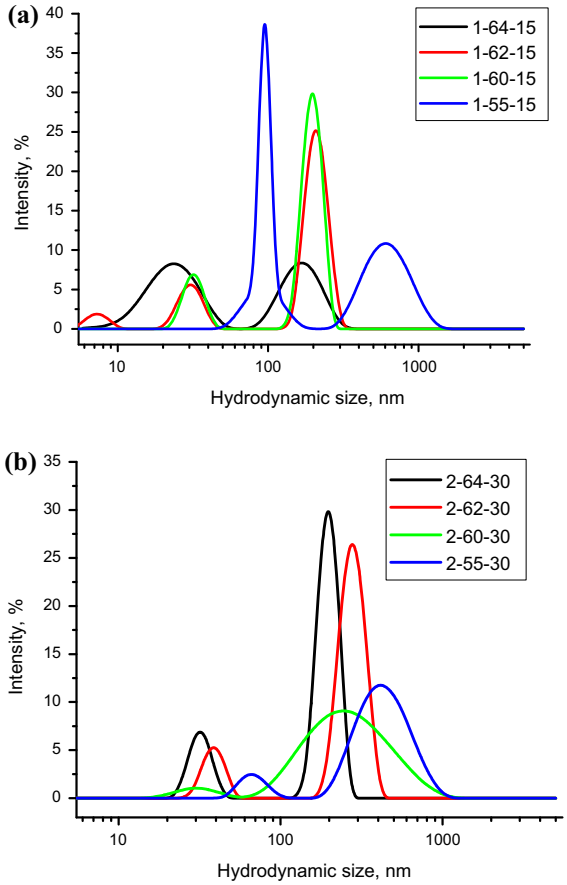

Fig. 5 Dynamic light scattering data for the CNC particles produced from MCC in different processing formats: **a** mode 1, **b** mode 2

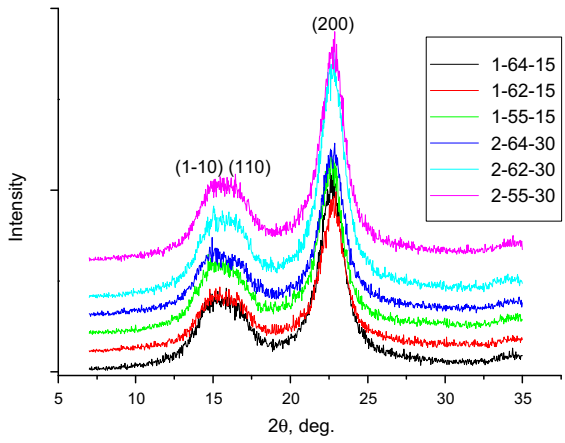

Fig. 6 X-ray diffraction patterns for films of the CNC produced from MCC in different processing formats

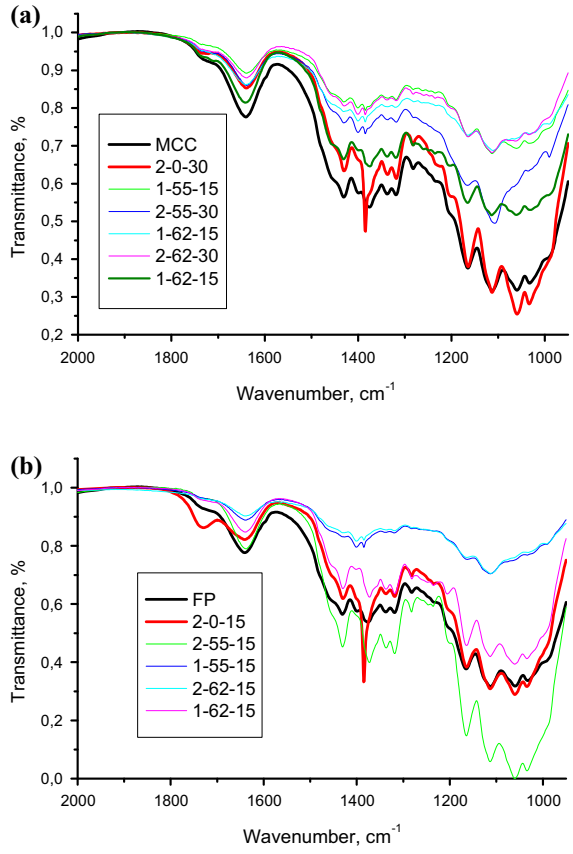

Fig. 7 IR spectra (in the range of 1000–2000 cm^{-1}) for MCC (**a**) and FP (**b**) samples after solution plasma treatment in different processing formats. For comparison, the spectra of MCC and FP before processing are given

XPS analysis was employed to analyze the CNC surface modifications taking place during the solution plasma treatment (Table 3) as well. The obtained C_{1s} XPS spectra consist of several components with different binding energy depending on the carbon oxidation degree (Supporting Information, Fig. 1S).

Pure cellulose exhibits two peaks in its deconvoluted C_{1s} XPS spectra: C–O of hydroxy and ethers groups with the binding energy of about 287 eV (83%) and O–C–O for hemiacetal moieties with the peak around 288 eV (17%) (Jiang et al. 2010; NIST Chemistry WebBook). In practice, the XPS analysis of cellulose always reveals three or even four peaks at about 285, 287, 288 and 289 eV, attributed to aliphatic or aromatic carbon (C–C/C–H), carbon in hydroxy and ethers groups (C–O), carbon in acetal fragments and/or carbonyl groups (O–C–O and/or C=O) and carbon in carboxyl groups (O–C=O), respectively (Gaiolas

et al. 2009; Pertile et al. 2010; Lu et al. 2015; Johansson and Campbell 2004; Espino-Pérez et al. 2014). The unexpected peak at about 285 corresponds to a contamination of the cellulose surface and is attributed to the impurities associated with the presence of residual aliphatic or aromatic carbon. According to Carlsson and Ström (1991), the carbon composition determined using filter paper, as given by XPS measurements, was found to be (8:72:17:3).

Analyzing the data of Table 3, it can be concluded that the relative content of oxygen and carbon as well as carbonyl and carboxyl groups for the CNC produced in various modes of plasma-chemical treatment are comparable.

The peak arising at 285 eV is probably due to products of cellulose oxidation and hydrolysis. It is worth noting that this peak has the lowest intensity for the control sample (produced by the standard hydrolysis procedure). It should also be noted that the solution plasma treatment of the CNC suspensions (mode 3) does not cause any noticeable changes in the properties of the CNC (Table 2, 3).

At a higher sulfuric acid concentration (62–64%), solution plasma treatment leads to practically complete hydrolysis of cellulose with formation of water-soluble products, as well as their further oxidation and destruction (as indicated by a noticeable change in color of the solution). Additionally, as the intensity of plasma solution treatment increases, the intensity of the color of the solution rises from weak pale yellow to yellow-brown (Table 1).

Figure 8 represents the absorption spectrum of water-soluble products formed during plasma-chemical treatment of MCC (processing format 1-62-15). For comparison, the spectrum of aqueous CNC suspension is shown. A similar yellow color of the aqueous phase recovered after hydrolysis of the oxidized cellulose was observed by Zhou et al. (2015), Chávez-Guerrero et al. (2018) as well.

Thus, cellulose degradation is accompanied by yellowing as the main consequence of hydrolysis and oxidation. The latter causes the development of functional groups which act as chromophores and are responsible for yellowing (Mosca Conte et al. 2012).

We have tried to identify the water-soluble products of cellulose oxidation and hydrolysis by analyzing the IR spectra of these products after their preliminary extraction by ethanol-toluene mixture and careful drying. Figure 9 shows the IR spectra of two of such samples.

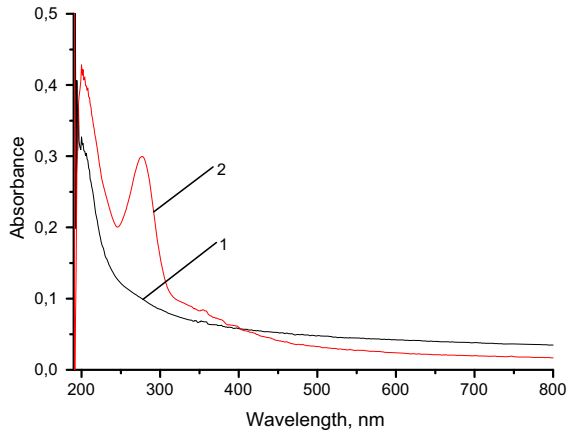

Fig. 8 UV-Vis spectrum of water-soluble products formed as a result of plasma-chemical treatment of MCC (processing format 1-62-15) (curve 2). For comparison, the spectrum of aqueous CNC suspension is shown (curve 1)

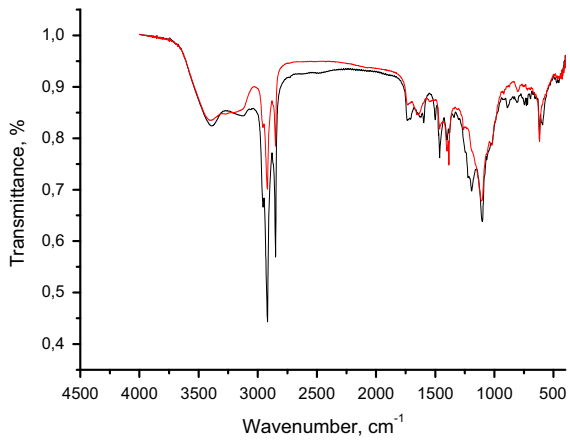

Fig. 9 IR spectra of the two samples of water-soluble cellulose oxidation and hydrolysis products

Comparing the IR spectra of the water-soluble products of solution plasma processing with the spectra of possible products of cellulose oxidation and hydrolysis (Bikales and Segal 1971; Rogovin 1972; Niu et al. 2015; Łojewski et al. 2010), we have come to a conclusion that the products of the plasma treatment are most probably a mixture of D-glucose with products of its further oxidation and hydrolysis (mainly, 5-(hydroxymethyl)furfural (HMF) and levulinic acid) (Spectral Database for Organic Compound SDBS). NMR spectra of the water-soluble products also confirm this (Supporting Information, Fig. 2S).

Conclusions

In this work, we have used, for the first time, solution plasma processing of cellulose-containing material (MCC and FP) to produce CNC. We have shown that solution plasma treatment in distilled water leads to cellulose oxidation and formation of surface carboxyl groups. However, in sulfuric acid solutions, the oxidation process is accompanied by hydrolysis. As a result of subsequent hydrolysis, the oxidized cellulose is mainly converted to water-soluble products, promoting the release of CNC particles. It was revealed that preliminary solution plasma treatment of cellulose followed by sulfuric acid hydrolysis almost doubles the yield of CNC (up to 56%) when the starting material is MCC.

Acknowledgments This work was supported by the Russian Science Foundation (Grant Number 17-13-01240). The authors would like to thank The Upper Volga Region Centre of Physicochemical Research (Ivanovo, Russia) and Centre for collective use of scientific equipment of Ivanovo State University of Chemistry and Technology for some measurements carried out using the centers' equipment.

Compliance with ethical standards

Conflict of interest None.

References

Araki J, Wada M, Kuga S, Okano T (1998) Flow properties of microcrystalline cellulose suspension prepared by acid treatment of native cellulose. Colloids Surf A 142:75–82. https://doi.org/10.1016/S0927-7757(98)00404-X

Beck-Candanedo S, Roman M, Gray DG (2005) Effect of reaction conditions on the properties and behavior of wood cellulose nanocrystal suspensions. Biomacromol 6:1048–1054. https://doi.org/10.1021/bm049300p

Bikales NM, Segal L (1971) Cellulose and cellulose derivatives. Wiley, New York

Bondeson D, Matthew A, Oksman K (2006) Optimization of the isolation of nanocrystals from microcrystalline cellulose by acid hydrolysis. Cellulose 13:171–180. https://doi.org/10.1007/s10570-006-9061-4

Braun B, Dorgan JR (2008) Single-step method for the isolation and surface functionalization of cellulosic nanowhiskers. Biomacromolecules 10(2):334–341. https://doi.org/10.1021/bm8011117

Camarero Espinosa S, Kuhnt T, Foster EJ, Weder C (2013) Isolation of thermally stable cellulose nanocrystals by phosphoric acid hydrolysis. Biomacromol 14(4):1223–1230. https://doi.org/10.1021/bm400219u

Carlsson CMG, Ström G (1991) Reduction and oxidation of cellulose surfaces by means of cold-plasma. Langmuir 7(11):2492–2497. https://doi.org/10.1021/la00059a016

Chávez-Guerrero L, Sepúlveda-Guzmán S, Silva-Mendoza J, Aguilar-Flores C, Pérez-Camacho O (2018) Eco-friendly isolation of cellulose nanoplatelets through oxidation under mild conditions. Carbohydr Polym 181:642–649. https://doi.org/10.1016/j.carbpol.2017.11.100

Chen L, Wang Q, Hirth K, Baez C, Agarwal UP, Zhu JY (2015) Tailoring the yield and characteristics of wood cellulose nanocrystals (CNC) using concentrated acid hydrolysis. Cellulose 22(3):1753–1762. https://doi.org/10.1007/s10570-015-0615-1

Chen L, Zhu JY, Baez C, Kitin P, Elder T (2016a) Highly thermal-stable and functional cellulose nanocrystals and nanofibrils produced using fully recyclable organic acids. Green Chem 18:3835–3843. https://doi.org/10.1039/C6GC00687F

Chen YW, Lee HV, Hamid SBA (2016b) Preparation and characterization of cellulose crystallites via Fe(III)-, Co(II)- and Ni(II)-assisted dilute sulfuric acid catalyzed hydrolysis process. J Nano Res 41:96–109. https://doi.org/10.4028/www.scientific.net/JNanoR.41.96

Cheng M, Qin Z, Chen Y, Hu S, Ren Z, Zhu M (2017) Efficient extraction of cellulose nanocrystals through hydrochloric acid hydrolysis catalyzed by inorganic chlorides under hydrothermal conditions. ACS Sustain Chem Eng 5(6):4656–4664. https://doi.org/10.1021/acssuschemeng.6b03194

Dong XM, Revol J-F, Gray DG (1998) Effect of microcrystallite preparation conditions on the formation of colloid crystals of cellulose. Cellulose 5(1):19–32. https://doi.org/10.1023/A:1009260511939

Espino-Pérez E, Domenek S, Belgacem N, Sillard C, Bras J (2014) Green process for chemical functionalization of nanocellulose with carboxylic acids. Biomacromol 15(12):4551–4560. https://doi.org/10.1021/bm5013458

Filson PB, Dawson-Andoh BE (2009) Sono-chemical preparation of cellulose nanocrystals from lignocellulose derived materials. Bioresour Technol 100(7):2259–2264. https://doi.org/10.1016/j.biortech.2008.09.062

Filson PB, Dawson-Andoh B, Schwegler-Berry D (2009) Enzymatic-mediated production of cellulose nanocrystals from recycled pulp. Green Chem 11:1808–1814. https://doi.org/10.1039/b915746h

French AD (2014) Idealized powder diffraction patterns for cellulose polymorphs. Cellulose 21(2):885–896. https://doi.org/10.1007/s10570-013-0030-4

Gaiolas C, Belgacem MN, Silva L, Thielemans W, Costa AP, Nunes M, Silva MJS (2009) Green chemicals and process to graft cellulose fibers. J Colloid Interf Sci 330(2):298–302. https://doi.org/10.1016/j.jcis.2008.10.059

Hamad WY, Hu TQ (2010) Structure-process-yield interrelations in nanocrystalline cellulose extraction. Can J Chem Eng 88(3):392–402. https://doi.org/10.1002/cjce.20298

Hirosawa S, Minato K, Nakatsubo F (2001) Influence of carboxyl group on the acid hydrolysis of cellulose. J Wood Sci 47(2):141–144. https://doi.org/10.1007/BF00780563

Hirota M, Furihata K, Saito T, Kawada T, Isogai A (2010a) Glucose/glucuronic acid alternating co-polysaccharides

prepared from TEMPO-oxidized native celluloses by surface peeling. Angew Chem Int Ed 49(42):7670–7672. https://doi.org/10.1002/anie.201003848

Hirota M, Tamura N, Saito T, Isogai A (2010b) Water dispersion of cellulose II nanocrystals prepared by TEMPO-mediated oxidation of mercerized cellulose at pH 4.8. Cellulose 17(2):279–288. https://doi.org/10.1007/s10570-009-9381-2

Ioelovich M (2012) Optimal conditions for isolation of nanocrystalline cellulose particles. Nanosci Nanotechnol 2(2):9–13. https://doi.org/10.5923/j.nn.20120202.03

Ioelovich M (2013) Products of cellulose hydrolysis made by treatment of feedstock with concentrated solutions of sulfuric acid. Res Rev J Mater Sci 1(1):12–19. https://doi.org/10.4172/2321-6212.1000103

Ioelovich M (2017) Characterization of various kinds of nanocellulose. In: Kargarzadeh H, Ahmad I, Thomas S, Dufresne A (eds) Handbook of nanocellulose and cellulose nanocomposites, 1st edn. Wiley, New York, pp 51–100. https://doi.org/10.1002/9783527689972.ch2

Jiang F, Esker AR, Roman M (2010) Acid-catalyzed and solvolytic desulfation of H_2SO_4-hydrolyzed cellulose nanocrystals. Langmuir 26(23):17919–17925. https://doi.org/10.1021/la1028405

Johansson L-S, Campbell JM (2004) Reproducible XPS on biopolymers: cellulose studies. Surf Interface Anal 36:1018–1022. https://doi.org/10.1002/sia.1827

Julkapli NM, Bagheri S (2017) Progress on nanocrystalline cellulose biocomposites. React Funct Polym 112:9–21. https://doi.org/10.1016/j.reactfunctpolym.2016.12.013

Kargarzadeh H, Ioelovich M, Ahmad I, Thomas S, Dufresne A (2017) Methods for extraction of nanocellulose from various sources. In: Kargarzadeh H, Ahmad I, Thomas S, Dufresne A (eds) Handbook of nanocellulose and cellulose nanocomposites, 1st edn. Wiley, New York, pp 1–49. https://doi.org/10.1002/9783527689972.ch1

Karim MZ, Chowdhury ZZ, Hamid SBA, Ali ME (2014) Statistical optimization for acid hydrolysis of microcrystalline cellulose and its physiochemical characterization by using metal ion catalyst. Materials 7:6982–6999. https://doi.org/10.3390/ma7106982

Khelifa F, Ershov S, Habibi Y, Snyders R, Dubois P (2016) Free-radical-induced grafting from plasma polymer surfaces. Chem Rev 116(6):3975–4005. https://doi.org/10.1021/acs.chemrev.5b00634

Kontturi E, Meriluoto A, Penttilä PA, Baccile N, Malho J-M, Potthast A, Rosenau T, Ruokolainen J, Serimaa R, Laine J, Sixta H (2016) Degradationand crystallization of cellulose in hydrogen chloride vapor for high-yield isolation of cellulose nanocrystals. Angew Chem Int Ed 55(46):14455–14458. https://doi.org/10.1002/anie.201606626

Kuz'micheva LA, Titova YV, Maksimov AI (2011) Yields of hydroxyl radicals and hydrogen peroxide in a glow discharge system with a liquid cathode. Surf Eng Appl Elect 47(6):45–47. https://doi.org/10.3103/S106837551106010X

Kuz'micheva LA, Titova YV, Maksimov AI (2012) Accumulation of hydrogen peroxide at the long-term effect of an atmosphere pressure glow discharge on electrolyte solutions. Surf Eng Appl Elect 48(1):60–63. https://doi.org/10.3103/S1068375512010103

Leung ACW, Hrapovic S, Lam E, Liu Y, Male KB, Mahmoud KA, Luong JHT (2011) Characteristics and properties of carboxylated cellulose nanocrystals prepared from a novel one-step procedure. Small 7(3):302–305. https://doi.org/10.1002/smll.201001715

Li J, Zhang X, Zhang M, Xiu H, He H (2015) Ultrasonic enhance acid hydrolysis selectivity of cellulose with HCl–$FeCl_3$ as catalyst. Carbohydr Polym 117:917–922. https://doi.org/10.1016/j.carbpol.2014.10.028

Li Y, Liu Y, Chen W, Wang Q, Liu Y, Li J, Yu H (2016) Facile extraction of cellulose nanocrystal from wood using ethanol and peroxide solvothermal pretreatment followed by ultrasonic nanofibrillation. Green Chem 18:1010–1018. https://doi.org/10.1039/C5GC02576A

Lin N, Dufresne A (2014) Surface chemistry, morphological analysis and properties of cellulose nanocrystals with gradiented sulfation degrees. Nanoscale 6:5384–5393. https://doi.org/10.1039/c3nr06761k

Liu L, Sun J, Cai C, Wang S, Pei H, Zhang J (2009) Corn stover pretreatment by inorganic salts and its effects on hemicellulose and cellulose degradation. Bioresour Technol 100(23):5865–5871. https://doi.org/10.1016/j.biortech.2009.06.048

Liu D, Zhong T, Chang PR, Li K, Wu Q (2010) Starch composites reinforced by bamboo cellulosic crystals. Bioresour Technol 101(7):2529–2536. https://doi.org/10.1016/j.biortech.2009.11.058

Liu Y, Wang H, Yu G, Yu Q, Li B, Mu X (2014) A novel approach for the preparation of nanocrystalline cellulose by using phosphotungstic acid. Carbohyd Polym 110:415–422. https://doi.org/10.1016/j.carbpol.2014.04.040

Łojewski T, Zięba K, Knapik A, Bagniuk J, Lubańska A, Łojewska J (2010) Evaluating paper degradation progress. Cross-linking between chromatographic, spectroscopic and chemical results. Appl Phys A 100:809–821. https://doi.org/10.1007/s00339-010-5657-5

López-Linares JC, Romero I, Moya M, Cara C, Ruiz E, Castro E (2013) Pretreatment of olive tree biomass with $FeCl_3$ prior enzymatic hydrolysis. Bioresour Technol 128:180–187. https://doi.org/10.1016/j.biortech.2012.10.076

Lu P, Hsieh Y-L (2010) Preparation and properties of cellulose nanocrystals: rods, spheres, and network. Carbohydr Polym 82:329–336. https://doi.org/10.1016/j.carbpol.2010.04.073

Lu Q, Tang L, Lin F, Wang S, Chen Y, Chen X, Huang B (2014) Preparation and characterization of cellulose nanocrystals via ultrasonication-assisted $FeCl_3$-catalyzed hydrolysis. Cellulose 21(5):3497–3506. https://doi.org/10.1007/s10570-014-0376-2

Lu Q, Li X, Tang L, Lu B, Huang B (2015) One-pot tandem reactions for the preparation of esterified cellulose nanocrystals with 4-dimethylaminopyridine as a catalyst. RSC Adv 5:56198–56204. https://doi.org/10.1039/c5ra08690f

Man Z, Muhammad N, Sarwono A, Bustam MA, Kumar MV, Rafiq S (2011) Preparation of cellulose nanocrystals using an ionic liquid. J Polym Environ 19(3):726–731. https://doi.org/10.1007/s10924-011-0323-3

Mao J, Abushammala H, Brown N, Laborie M-P (2017) Comparative assessment of methods for producing cellulose I nanocrystals from cellulosic sources. In: Agarwal UP, Atalla RH, Isogai A (eds) Nanocelluloses: their preparation, properties, and applications, ACS symposium series, vol 1251. American Chemical Society, Washington, pp 19–53. https://doi.org/10.1021/bk-2017-1251.ch002

Miao J, Yu Y, Jiang Z, Zhang L (2016) One-pot preparation of hydrophobic cellulose nanocrystals in an ionic liquid. Cellulose 23(2):1209–1219. https://doi.org/10.1007/s10570-016-0864-7

Mondal S (2017) Preparation, properties and applications of nanocellulosic materials. Carbohyd Polym 163:301–316. https://doi.org/10.1016/j.carbpol.2016.12.050

Montanari S, Roumani M, Heux L, Vignon MR (2005) Topochemistry of carboxylated cellulose nanocrystals resulting from TEMPO-mediated oxidation. Macromolecules 38(5):1665–1671. https://doi.org/10.1021/ma048396c

Mosca Conte A, Pulci O, Knapik A, Bagniuk J, Del Sole R, Lojewska J, Missori M (2012) Role of cellulose oxidation in the yellowing of ancient paper. Phys Rev Lett 108:158301. https://doi.org/10.1103/PhysRevLett.108.158301

Nikitin D, Choukourov A, Titov V, Kuzmicheva L, Lipatova I, Mezina E, Aleksandriiskii V, Shelemin A, Khalakhan I, Slavinska D, Biederman H (2016) In situ coupling of chitosan onto polypropylene foils by an Atmospheric Pressure Air Glow Discharge with a liquid cathode. Carbohydr Polym 154:30–39. https://doi.org/10.1016/j.carbpol.2016.08.023

NIST Chemistry WebBook, http://webbook.nist.gov/chemistry. Accessed 01 Feb 2018

Niu M, Hou Y, Ren S, Wang W, Zheng Q, Wu W (2015) The relationship between oxidation and hydrolysis in the conversion of cellulose in $NaVO_3$–H_2SO_4 aqueous solution with O_2. Green Chem 17:335–342. https://doi.org/10.1039/c4gc00970c

Novo LP, Bras J, García A, Belgacem N, Curvelo AAS (2015) Subcritical water: a method for green production of cellulose nanocrystals. ACS Sustain Chem Eng 3(11):2839–2846. https://doi.org/10.1021/acssuschemeng.5b00762

Novo LP, Bras J, García A, Belgacem N, Curvelo AAS (2016) A study of the production of cellulose nanocrystals through subcritical water hydrolysis. Ind Crop Prod 93:88–95. https://doi.org/10.1016/j.indcrop.2016.01.012

Pertile RAN, Andrade FK, Alves C Jr, Gama M (2010) Surface modification of bacterial cellulose by nitrogen-containing plasma for improved interaction with cells. Carbohydr Polym 82:692–698. https://doi.org/10.1016/j.carbpol.2010.05.037

Peyre J, Pääkkönen T, Reza M, Kontturi E (2015) Simultaneous preparation of cellulose nanocrystals and micron-sized porous colloidal particles of cellulose by TEMPO-mediated oxidation. Green Chem 17:808–811. https://doi.org/10.1039/C4GC02001D

Piotto M, Saudek V, Sklenář V (1992) Gradient-tailored excitation for single-quantum NMR spectroscopy of aqueous solutions. J Biomol NMR 2(6):661–665. https://doi.org/10.1007/BF02192855

Prasertsunga I, Chutinate P, Watthanaphanit A, Saito N, Damrongsakkul S (2017) Conversion of cellulose into reducing sugar by solution plasma process (SPP). Carbohydr Polym 172:230–236. https://doi.org/10.1016/j.carbpol.2017.05.025

Rogovin ZA (1972) Chemistry of cellulose. Khimia, Moscow (in Russian)

Siqueira G, Tapin-Lingua S, Bras J, da Silva Perez D, Dufresne A (2010) Morphological investigation of nanoparticles obtained from combined mechanical shearing, and enzymatic and acid hydrolysis of sisal fibers. Cellulose 17(6):1147–1158. https://doi.org/10.1007/s10570-010-9449-z

Spectral Database for Organic Compound SDBS. National Institute of Advanced Industrial Science and Technology (AIST), http://sdbs.db.aist.go.jp. Accessed 01 Feb 2018

Spinella S, Maiorana A, Qian Q, Dawson NJ, Hepworth V, McCallum SA, Ganesh M, Singer KD, Gross RA (2016) Concurrent cellulose hydrolysis and esterification to prepare a surface-modified cellulose nanocrystal decorated with carboxylic acid moieties. ACS Sustain Chem Eng 4(3):1538–1550. https://doi.org/10.1021/acssuschemeng.5b01489

Titiova YV, Voronova MI, Maksimov AI (2008) Influence of gas-discharge plasma treatment in the electrolyte bulk on the cellulose properties. Russ J Appl Chem 81(5):854–857. https://doi.org/10.1134/s107042720805025x

Titova YV, Stokozenko VG, Aleksakhina EL, Maksimov AI (2012) Chemical interactions of a model lignin compound under plasma-solution treatment. Surf Eng Appl Elect 48(4):355–358. https://doi.org/10.3103/S1068375512040175

Torlopov MA, Udoratina EV, Maratov IS, Sitnikov PA (2017a) Cellulose nanocrystals prepared in $H_3PW_{12}O_{40}$-acetic acid system. Cellulose 24(5):2153–2162. https://doi.org/10.1007/s10570-017-1256-3

Torlopov MA, Mikhaylov VI, Udoratina EV, Aleshina LA, Prusskii AI, Tsvetkov NV, Krivoshapkin PV (2017b) Cellulose nanocrystals with different length-to-diameter ratios extracted from various plants using novel system acetic acid/phosphotungstic acid/octanol-1. Cellulose 25(2):1031–1046. https://doi.org/10.1007/s10570-017-1624-z

Um BH, Karim MN, Henk LL (2003) Effect of sulfuric and phosphoric acid pretreatments on enzymatic hydrolysis of corn stover. Appl Biochem Biotechnol 105–108(1–3):115–125. https://doi.org/10.1385/ABAB:105:1-3:115

Voronova MI, Surov OV, Guseinov SS, Barannikov VP, Zakharov AG (2015) Thermal stability of polyvinyl alcohol/nanocrystalline cellulose composites. Carbohydr Polym 130:440–447. https://doi.org/10.1016/j.carbpol.2015.05.032

Wang QQ, Zhu JY, Reiner RS, Verrill SP, Baxa U, McNeil SE (2012) Approaching zero cellulose loss in cellulose nanocrystal (CNC) production: recovery and characterization of cellulosic solid residues (CSR) and CNC. Cellulose 19(6):2033–2047. https://doi.org/10.1007/s10570-012-9765-6

Yahya M, Lee HV, Hamid SBA (2015) Preparation of nanocellulose via transition metal salt-catalyzed hydrolysis

pathway. BioResources 10(4):7627–7639. https://doi.org/10.15376/biores.10.4.7627-7639

Yan C-F, Yu H-Y, Yao J-M (2015) One-step extraction and functionalization of cellulose nanospheres from lyocell fibers with cellulose II crystal structure. Cellulose 22(6):3773–3788. https://doi.org/10.1007/s10570-015-0761-5

Yu H, Qin Z, Liang B, Liu N, Zhou Z, Chen L (2013) Facile extraction of thermally stable cellulose nanocrystals with a high yield of 93% through hydrochloric acid hydrolysis under hydrothermal conditions. J Mater Chem A 1(12):3938–3944. https://doi.org/10.1039/C3TA01150J

Zakharov AG, Maksimov AI, Titova YV (2007) Physicochemical properties of plasma–solution systems and prospects for their use in technology. Russ Chem Rev 76(3):235–251. https://doi.org/10.1070/RC2007v076n03ABEH003638

Zhang Y, Li Q, Su J, Lin Y, Huang Z, Lu Y, Sun G, Yang M, Huang A, Hu H, Zhu Y (2015) A green and efficient technology for the degradation of cellulosic materials: structure changes and enhanced enzymatic hydrolysis of natural cellulose pretreated by synergistic interaction of mechanical activation and metal salt. Bioresour Technol 177:176–181. https://doi.org/10.1016/j.biortech.2014.11.085

Zhang J, Wu J, Yu J, Zhang X, He J, Zhang J (2017) Application of ionic liquids for dissolving cellulose and fabricating cellulose-based materials: state of the art and future trends. Mater Chem Front 1(7):1273–1290. https://doi.org/10.1039/C6QM00348F

Zhou L, Yang X, Xu J, Shi M, Wang F, Chen C, Xu J (2015) Depolymerization of cellulose to glucose by oxidation–hydrolysis. Green Chem 17:1519–1524. https://doi.org/10.1039/c4gc02151g

Zhu H, Luo W, Ciesielski PN, Fang Z, Zhu JY, Henriksson G, Himmel ME, Hu L (2016) Wood-derived materials for green electronics, biological devices, and energy applications. Chem Rev 116:9305–9374. https://doi.org/10.1021/acs.chemrev.6b00225